

Hybrid Lithographic and DNA-Directed Assembly of a Configurable Plasmonic Metamaterial That Exhibits Electromagnetically Induced Transparency

David B. Litt,^{†,‡,§,||,⊥} Matthew R. Jones,^{†,||} Mario Hentschel,[‡] Ying Wang,^{||,‡} Sui Yang,^{||,‡} Hyun Dong Ha,^{†,‡} Xiang Zhang,^{||,‡,§,⊥,||} and A. Paul Alivisatos^{*,†,‡,§,⊥,||}

[†]Department of Chemistry, University of California, Berkeley, California 94720, United States

[‡]Materials Sciences Division, Lawrence Berkeley National Laboratory, Berkeley, California 94720, United States

[§]Department of Materials Science and Engineering, University of California, Berkeley, California 94720, United States

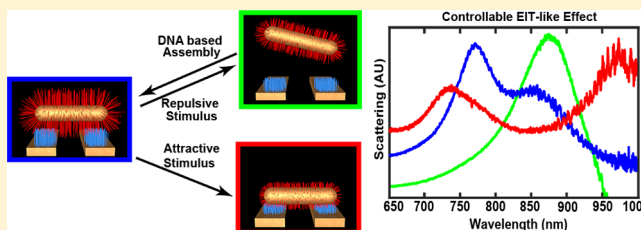
^{||}Nanoscale Science and Engineering Center, University of California, Berkeley, California 94720, United States

[⊥]Kavli Energy NanoScience Institute, Berkeley, California 94720, United States

Supporting Information

ABSTRACT: Metamaterials are architectures that interact with light in novel ways by virtue of symmetry manipulation, and have opened a window into studying unprecedented light-matter interactions. However, they are commonly fabricated via lithographic methods, are usually static structures, and are limited in how they can react to external stimuli. Here we show that by combining lithographic techniques with DNA-based self-assembly methods, we can construct responsive plasmonic metamaterials that exhibit the plasmonic analog of an effect known as electromagnetically induced transparency (EIT), which can dramatically change their spectra upon motion of their constituent parts. Correlative scanning electron microscopy measurements, scattering dark-field microscopy, and computational simulations are performed on single assemblies to determine the relationship between their structures and spectral responses to a variety of external stimuli. The strength of the EIT-like effect in these assemblies can be tuned by precisely controlling the positioning of the plasmonic nanoparticles in these structures. For example, changing the ionic environment or dehydrating the sample will change the conformation of the DNA linkers and therefore the distance between the nanoparticles. Dark-field spectra of individual assemblies show peak shifts of up to many tens of nanometers upon DNA perturbations. This dynamic metamaterial represents a stepping stone toward state-of-the-art plasmonic sensing platforms and next-generation dynamic metamaterials.

KEYWORDS: Metamaterials, DNA, self-assembly, nanoparticles, plasmonics, electromagnetically induced transparency



Optical metamaterials consist of subwavelength dielectric or plasmonic structures that manipulate light in profound, often surprising, and even unnatural ways, allowing for novel phenomena such as negative index of refraction and invisibility cloaks.^{1–10} In many cases, these properties arise only when the individual building blocks (the meta-atoms) consist of a low-symmetry arrangement of inorganic components. By correctly designing the arrangement of these components, one can program the manner in which they interact with light. To achieve the requisite broken symmetries to create a metamaterial, lithographic methods are frequently employed, as they allow for nearly arbitrary pattern formation in two and to some degree in three dimensions. However, the resulting structures are usually static and can rarely change in response to external stimuli. Constructing a dynamic metamaterial that responds to local environmental changes would be advantageous for many reasons, for example, by allowing a metamolecule to autonomously shift the frequency of its

resonant mode for optical mode selection and as a sensing modality.^{11–17}

Self-assembly offers an attractive route to achieving materials that can change their structure and subsequent properties because the forces that govern their formation are generally weak (on the order of a few kT) and can respond to external stimuli in a rich multitude of ways and with enormous selectivity.^{18–22} Unfortunately, these interactions, without designed symmetry manipulations, do not possess metamaterial-like properties. Here we show, through a combination of lithographic templating and DNA-directed self-assembly, the formation of a plasmonic metamaterial capable of responding to its environment by changing its structural configuration. As a model three-dimensional system, we have synthesized a structure consisting of three gold rods that, when properly

Received: September 25, 2017

Revised: December 12, 2017

Published: January 5, 2018

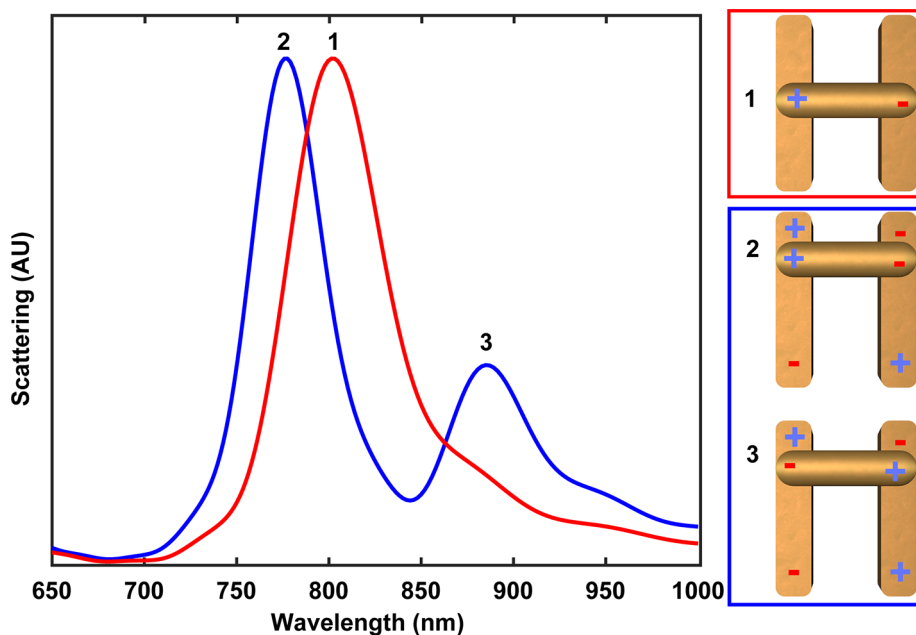


Figure 1. Dipole-based explanation of the plasmonic analog to electromagnetically induced transparency (EIT). FDTD simulations were run of the low and high symmetry assemblies with incident light linearly polarized along the longitudinal axis of the orthogonal rod. The parallel rods are simulated to be $115 \times 35 \times 30$ nm with a 30 nm gap between them, and the orthogonal rod is 96×30 nm with a 15 nm gap above the parallel rods. A symmetrical assembly (top, red box) in which an orthogonal rod assembles across the center of the parallel rods will have a single peak (1) in the scattering spectrum (red trace) because the orthogonal rod is in the node of the quadrupolar resonance and will not couple with it. An unsymmetrical assembly (middle and bottom, blue box) exhibits an EIT-like response (blue trace) because the dipole mode from the orthogonal rod can couple with the quadrupolar mode from the parallel rods, giving rise to two new coupled collective modes (peaks 2 and 3). Note that the transparency window is in a similar position to the peak of the symmetric structure.

arranged, exhibits a plasmonic analogue of an optical phenomenon known as electromagnetically induced transparency (EIT).^{23–25} By introducing stimuli that perturb the conformation of the DNA linkers, individual elements of each assembly alter their configurations, changing the resonant modes of the constructed metamaterials. Our observation has been confirmed by correlating dark-field microscopy, scanning electron microscopy, and finite difference time domain simulations (FDTD) at the single meta-atom level. We anticipate that this work will open the door to creating dynamic and complex metamaterials that could switch their optical behavior in response to a variety of chemical stimuli.

Previous efforts to create dynamic metamaterials have focused on electrical, optical, or mechanical approaches to modulate the relevant optical modes of the system. For example, dielectric shifts via nearby phase-change materials, mechanical deformation of an underlying substrate, and charge-carrier injection via ultrafast optical pulses have all been used as stimuli to influence metamaterial properties.^{26–29} However, the use of chemical stimuli to drive similar structural and optical changes are considerably less common but important. For instance, a chemical stimulus would allow for the metamaterial to be manipulated in a substrate independent manner and, depending on how the chemical interaction modulates the mode coupling strength, the metamaterial could be manipulated to different degrees in order to tune magnitude of the response.

A particularly appealing method to create dynamic nanostructures that respond to chemical stimuli is to use organic linkers such as DNA to self-assemble the individual plasmonic nanoparticles components.^{20,30–34} Being molecular in nature, these linkers can be designed to respond to specific

binding events or general environmental changes. Previously, the Alivisatos group has developed so-called “plasmon rulers” that modulate the distance between two DNA-linked gold nanoparticles via small molecule interactions.^{35–38} In addition, the Mirkin group has shown the crystallization of DNA-functionalized nanoparticles into superlattices that can dynamically rearrange based on the presence of different oligonucleotide stimuli.^{18,19,39} However, in both cases the assemblies are highly symmetric and lack the structural complexity necessary to support metamaterial behavior. DNA origami techniques offer a potential route to address this shortcoming, as they allow for the folding of long DNA strands into low-symmetry 3D templates, on which nanoparticles can be selectively placed and dynamically switched via exogenous chemical stimuli. For instance, the Liedl and Liu groups have both used separate DNA origami-based strategies to create chiral assemblies, some of which can switch handedness when the appropriate oligonucleotide effector strand is introduced.^{17,40,41} However, these structures are assembled in a solution environment and thus are capable of supporting only orientationally averaged metamaterial properties. Because many metamaterials are fabricated on a substrate and have optical modes that require the excitation to be linearly polarized, methods to generate surface-based, self-assembled metamaterials are necessary. In this work, we show that by combining DNA-directed self-assembly with lithographically defined templates we can synthesize dynamic, low symmetry, plasmonic metamaterials that dramatically change their spectra upon introduction of a chemical stimulus.

Our model system is a metamaterial that exhibits EIT-like behavior.^{23–25,42,43} Briefly, EIT is a quantum interference effect seen in atomic systems, and leads to a sharp splitting in the

spectral signature of the atom that renders a transparent window, but an analogous (nonquantum) splitting effect can be seen in plasmonic systems and is referred to as EIT-like in this work.^{44,45} The structure consists of two parallel rods that together support a dark quadrupolar plasmon mode and a single orthogonal rod placed above them that supports a simple dipolar mode (Figure 1). If the orthogonal rod is centered in the middle of the parallel rods (a high symmetry arrangement), then its dipolar resonance will not couple into the dark quadrupolar resonance of the parallel rods. This results in a scattering spectrum with a single peak. On the other hand, if the orthogonal rod is offset and resides over the tips of the parallel rods (a low symmetry arrangement), its dipolar resonance will couple to the quadrupolar mode of the parallel rods. This results in a splitting of the peak into two separate modes, creating a transparency window in the optical spectrum. Assemblies exhibiting this EIT-like effect have been shown to be highly responsive to perturbations in their structure; even a few nanometer displacement in the relative positions of the rods can cause spectral shifts on the order of tens of nanometers.^{43,46–48} It has been theorized that if these structures were able to respond to external stimuli, the easily detected change in their spectra could be correlated to a configurational change and thus could have a strong impact as sensors across various fields.⁴³ This intrinsic sensitivity to structural changes makes the EIT-like design an ideal platform for investigating dynamic configuration in metamaterials defined by molecular self-assembled interactions.

To fabricate this structure in a manner that allows it to respond to chemical stimuli, we have implemented a combination of lithography and self-assembly to create a hybrid inorganic–organic architecture. The simple design of the EIT-like structure consisting of only three distinct rods also lends itself to this approach. First, the parallel rods defining the quadrupolar mode are fabricated on a conductive, transparent substrate using traditional lithography techniques. After spin coating poly(methyl methacrylate) (PMMA), a second layer exposure is then used to define a rod-shaped trench orthogonal to and above the parallel rods. This allows for DNA functionalization of the exposed area of the parallel rods which can subsequently be used to capture colloiddally synthesized rods functionalized with complementary DNA strands (Figure 2). Therefore, by introducing chemical stimuli that alter the conformation of the DNA the spacing (and therefore the degree of plasmonic coupling and the EIT-like response) between the parallel rods and the orthogonal rod can be postsynthetically tuned.

To validate this strategy for synthesizing hybrid metamaterials defined by lithography and self-assembly, we first generated static EIT-like structures with controlled asymmetry. Representative scanning electron microscopy (SEM) images illustrate that the lithographed trench can serve to direct the DNA functionalized orthogonal rods at desired positions along the length of the parallel rods (Figure 3). Note that electron microscopy images are collected under vacuum, resulting in dehydration of the DNA and collapse of the structure (see below).^{49,50} Nonetheless, placement of the orthogonal rod appears to be sufficiently precise so as to tailor the asymmetry of the structure. Detailed assembly results are enumerated in the SI and show the desired structures correctly self-assemble about 15 percent of the time and that the placement of the orthogonal rod along the parallel rods can be controlled with a standard deviation of ± 33 nm. To confirm that these materials

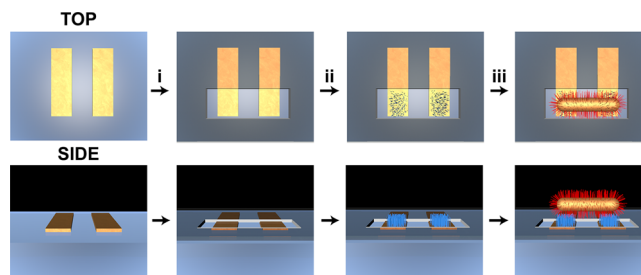


Figure 2. Schematic illustration of the lithography and assembly process of hybrid inorganic–organic structures. Parallel rods are first written on the indium tin oxide coated glass surface using e-beam lithography followed by gold evaporation. (i) A second layer exposure is done to open a trench over a specific position of the parallel rods, and a brief O₂ plasma etch is used to remove residual PMMA in the trench. (ii) Thiolated DNA (blue) is then added to the exposed portion of the parallel rods. (iii) Finally, the orthogonal rod functionalized with complementary DNA (red) is incubated on the glass slide, falls into the PMMA trench and hybridizes on the parallel rods.

indeed exhibit the desired EIT-like effect, single-particle dark-field scattering microscopy was used to measure the optical spectra of individual assemblies with the incident light polarized along the longitudinal axis of the orthogonal rod. Note that these spectra are acquired in a hydrated state and therefore preserve the DNA conformation and the resulting interparticle spacing defined by the number of bases in the strands. Consistent with theory and previous studies,²⁴ the degree of symmetry breaking determines the presence or absence of an EIT-like effect; symmetric structures show a single peak, whereas broken symmetry assemblies show two peaks with a transparency window. The spectra of individual assemblies are correlated with an SEM image after acquisition of the optical data (Figure 4); rods may appear angled in these images due to dehydration but are not necessarily oriented this way during the measurement while in solution. We find excellent agreement between the dark-field spectra data and finite difference time domain (FDTD) simulations of the assembly using structural parameters based on the SEM measurements, as is standard for these experiments.^{51,52}

To test if the presence of organic molecular components linking together the metamaterial could be used to post-synthetically modulate the structure, a flow cell setup was used to monitor the consequences of changing the chemical environment of the assemblies. Because a dense layer of hybridized DNA strands defines the spacing between the parallel rod and the orthogonal rods, chemical stimuli that alter the binding strength and conformation of the DNA can be used to modulate the structure. We first focused on changing the ionic strength of the solution to influence the ability or inability of the DNA to remain hybridized. Because DNA hybridization requires the presence of salt to screen the polyanionic phosphate backbone, lowering of the ionic strength via dilution with pure water will result in strand–strand repulsion and dehybridization.⁵³ To test this, assembled structures were hydrated in a high-salt buffer solution (~ 0.5 M ionic strength) and monitored via dark-field scattering microscopy while pure water with 0.01% sodium dodecyl sulfate (SDS) was flowed into the system. Initial structures showed the expected EIT-like behavior but dilution of the ionic strength by several orders of magnitude resulted in a loss of the peak splitting (Figure 5a,b). The dehybridization of the numerous DNA strands results in

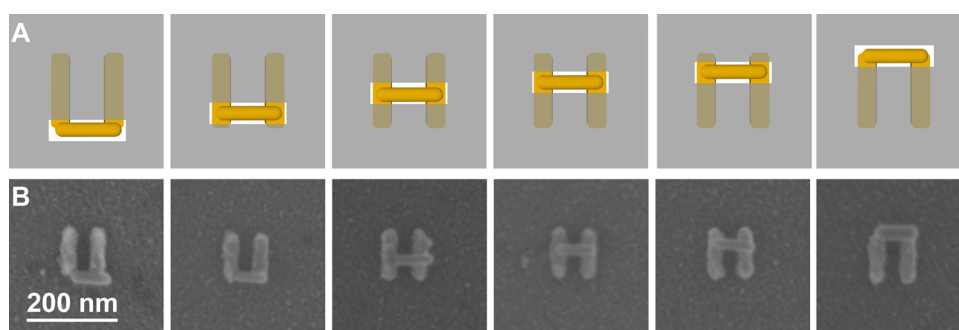


Figure 3. Symmetry control of inorganic–organic hybrid EIT-like structures. (a) Schematic showing the parallel rods covered in PMMA (gray) except for the trench opened by e-beam lithography over a specific location along the length of the parallel rods. (b) SEM images of assembled structures showing that the two layer exposure can direct assembly of the dipole rod along the length of the parallel rods. The PMMA is removed for SEM acquisition because it is insulating.

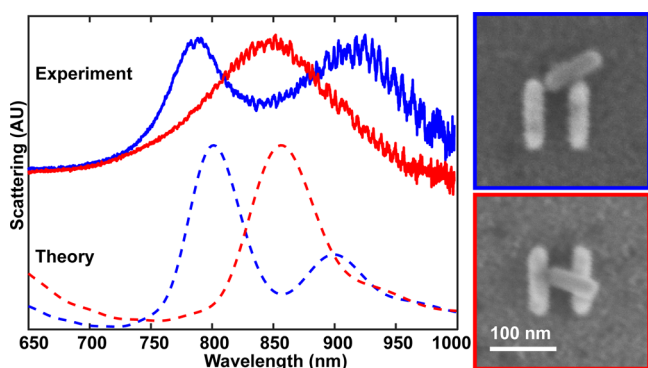


Figure 4. Correlative dark-field scattering microscopy and EM images of hybrid organic–inorganic EIT-like structures. The symmetric structure (red trace and red boxed SEM image) has a single peak. The low symmetry structure (blue trace and blue-boxed SEM image) exhibits the expected peak splitting indicative of the EIT-like effect. Dashed lines are FDTD simulations of the respective assemblies in hydrated states and show qualitative agreement with experiment (the traces are offset for clarity). The dimensions of the assemblies used in the simulations are extracted from the SEM images.

unbinding and removal of the colloiddally synthesized orthogonal rod and loss of the necessary plasmon coupling. The remaining single peak (red) is due to a coupled dipolar resonance from the parallel rods, as the quadrupole mode should be dark without the dipole rod. This shows the ability for a hybrid inorganic–organic metamaterial to switch between optically transparent and optically scattering states as a result of a change in the ionic strength of the environment based on plasmonic decoupling of the constituent parts.

We note that the presence of the red peak in Figure 5b is not predicted by the simulations with the incident light polarized orthogonal to the parallel rods; there should be no resonance from the orthogonal rod in the 650–1000 nm region, and when the orthogonal rod is removed, we would not expect to observe a spectral signal. However, a signal is always observed. There are several possibilities for this. First, in a transmission mode dark-field setup, the light is polarized orthogonal to the parallel rods (along the longitudinal axis of the orthogonal rod) before the light enters the dark-field condenser. Because of the arrangement of the mirrors in the condenser, it is impossible to perfectly preserve the polarization, and the dipolar mode of the parallel rods can be excited. Therefore, polarization is not perfect for high k components of the incident light, which is an intrinsic property of dark-field scattering spectroscopy. The

second possible reason is that the lithographed parallel rods are not identical. In fact, SEM imaging shows a couple nanometer difference in length and width for most pairs of parallel rods (data not shown), so the quadrupolar mode will not be entirely dark. Further explanations are explored in the Supporting Information. Taken together, these reasons likely explain the presence of the resonant mode of the parallel rods even though it would not be present under ideal conditions. Furthermore, when the spectral signal of the parallel rods is subtracted from that of the fully assembled structure, a very strong EIT-like effect is observed (black trace). This subtracted spectra most likely shows the true EIT-like signal of the correctly assembled structure when it is deconvoluted from the dipolar resonance of the parallel rods (Figure 5b).

Although changing ionic strength switches the behavior of the EIT-like structure, this perturbation is irreversible because the colloidal rod diffuses away and is unlikely to return to the same binding site even if appropriate salt conditions are reinstated. If instead, the distance between the components is modulated via a different chemical stimulus to bring the orthogonal rod closer to the parallel rods by perturbing the DNA conformation, an enhancement in the EIT-like effect can be observed. To probe this possibility, we investigated changes to the solvation environment and their influence on the hybrid metamaterial. EIT-like structures were prepared as described previously in a hydrated buffer solution. Although double-stranded DNA is a relatively rigid molecule in this state, upon dehydration and removal of the solvent, a collapsed and condensed conformation is adopted instead.^{49,54} Subjecting the system to vacuum and removing the water therefore results in a change in the spacing of the constituent rods (Figure 5c,d). In the case of our DNA strand design, the vertical gap between the orthogonal and parallel rods is expected to decrease from 15 nm for the hydrated case to about 5 nm for the dehydrated case.^{50,55} The resulting increase in plasmon coupling causes more pronounced splitting of the modes and a greater dip of the transparency window, as predicted by theory (using an effective index of 1.33 or that of water). The enhanced coupling and splitting in the spectra is a physical manifestation of the fact that the closer together the plasmonic nanoparticles are, the more the evanescent electromagnetic fields overlap and interact and are reflected in the spectral signature of the assembly. These data show how small changes in the conformation of molecules can be read-out as large changes in the optical spectra of a dynamic metamaterial.

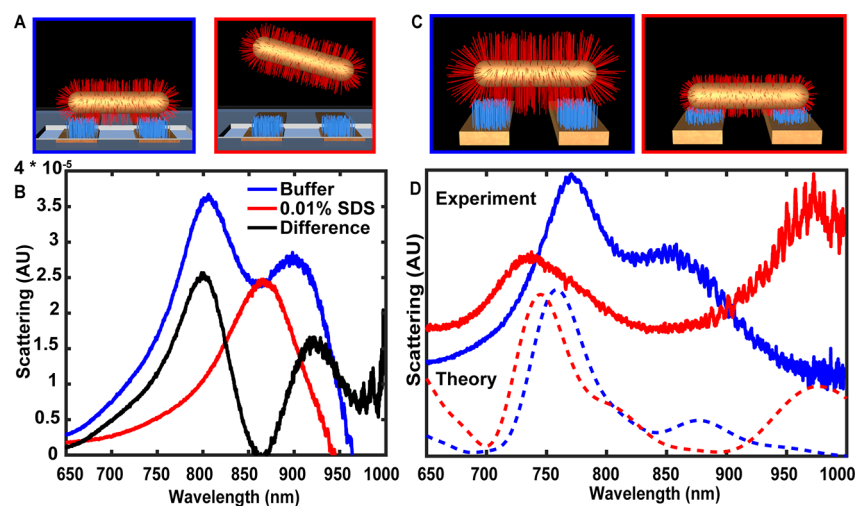


Figure 5. Dynamics of the hybrid inorganic–organic structure that exhibits an EIT-like effect. (a) Salt-based disassembly and destruction of EIT-like property due to changing ionic strength. The assembled structure in the blue box represents the structure in 0.5 M NaCl. The structure in the red box represents the disassembly in 0.01% SDS solution. (b) The blue trace is the measured dark-field EIT-like feature of an assembly taken in 0.5 M NaCl buffer. After flowing in water, a single peak of the same structure (red) is observed in dark-field imaging. This peak corresponds to the longitudinal resonance of the remaining parallel rods. The black trace is the difference of the two peaks and represents the true EIT-like effect of the assembled structure had the dipolar resonance of the parallel rods been completely suppressed. (c) Response to the hydration environment of the EIT-like assemblies. Side-on view of the hydrated state where the DNA is in its extended conformation (blue box). The DNA collapses upon removal of the solvent and dehydration (red box). (d) Dark-field spectra of the EIT-like assembly in its hydrated state (solid blue) and dry state (solid red). When the assembly is dehydrated, the rods come closer together, which will increase the magnitude of the EIT-like effect, broadening the transparency window. FDTD simulation of the hydrated state (dashed blue) and dry state (dashed red). Scattering intensity is normalized to make the shift in peak positions clear. The theory and experimental data are offset for clarity.

This work has demonstrated that it is possible to generate structures that combine the advantages of lithography to create low-symmetry metamaterials with those of self-assembly to create dynamic and flexible soft matter components. The organic elements provide a chemically responsive handle which can be rationally modulated by changes to the global environment. It should be noted that in this work the DNA was treated primarily as a traditional polymer; single assemblies were manipulated by bulk methods such as changing ionic strength or solvation environment. Future work will focus on using the sequence-specific binding properties of DNA to dynamically manipulate assembled metamaterials, for instance, by using strand displacement reactions. Such a design would impart an information processing element to the metamaterial switching and may allow this architecture to behave as a three-dimensional plasmon ruler that reports on complex biomolecule binding events via changes in the EIT-like spectrum. Ultimately, chemically dynamic metamaterials could be applicable to a host of fields that require structural reconfiguration to advance goals in optics, biological sensing, and materials science.

■ ASSOCIATED CONTENT

Supporting Information

The following files are available free of charge. Supporting Information (PDF) The Supporting Information is available free of charge on the ACS Publications website at DOI: 10.1021/acs.nanolett.7b04116.

Additional information, figures, and tables (PDF)

■ AUTHOR INFORMATION

Corresponding Author

*E-mail: paul.alivisatos@berkeley.edu.

ORCID

David B. Litt: 0000-0002-4338-1312

Matthew R. Jones: 0000-0002-9289-291X

Xiang Zhang: 0000-0002-3272-894X

A. Paul Alivisatos: 0000-0001-6895-9048

Notes

The authors declare no competing financial interest.

■ ACKNOWLEDGMENTS

This work was funded by the U.S. Department of Energy, Office of Science, Office of Basic Energy Sciences, Materials Sciences and Engineering Division under Contract No. DE-AC02-05-CH11231 within the Characterization of Functional Nanomachines Program, KC1203 (D.B.L., H.D.H, and lithography work) and within the Subwavelength Metamaterials Program, KC12XZ (S.Y., Y.W., and X.Z.). Optical modeling was supported by the Light-Material Interactions in Energy Conversion, an Energy Frontier Research Center funded by the U.S. Department of Energy, Office of Science, Office of Basic Energy Sciences, under Contract DE-AC02-05CH11231, part of the EFRC at Caltech under DE-SC0001293. The nanoparticle synthesis, the design of the linking DNA sequences, and the assembly work was supported by the National Science Foundation under Grant DMR-1344290. M.R.J. acknowledges the Arnold and Mabel Beckman Foundation for a postdoctoral fellowship. M.H. gratefully acknowledges financial support by the Alexander von Humboldt Foundation through a Feodor Lynen scholarship. We thank Dr. Alexander Koshelev at LBL and Dr. Kathy Durkin at the molecular graphics and computation facility at UC Berkeley (NIH S10OD023532) for help with Lumerical FDTD. D.L. would like to thank Xingchen Ye for productive conversations. We also thank Greg Mullins and Dr. Jeffery Clarkson for training on e-beam

lithography and SEM imaging. The authors acknowledge the Marvell Nanofabrication Laboratory for the use of their facilities.

REFERENCES

- (1) Liu, Y.; Zhang, X. *Chem. Soc. Rev.* **2011**, *40* (5), 2494–2507.
- (2) Shelby, R. A.; Smith, D. R.; Schultz, S. *Science* **2001**, *292* (5514), 77–79.
- (3) Linden, S.; Enkrich, C.; Wegener, M.; Zhou, J.; Koschny, T.; Soukoulis, C. M. *Science* **2004**, *306* (5700), 1351–1353.
- (4) Zhang, S.; Fan, W.; Panoiu, N. C.; Malloy, K. J.; Osgood, R. M.; Brueck, S. R. J. *Phys. Rev. Lett.* **2005**, *95* (13), 137404.
- (5) Pendry, J. B.; Shurig, D.; Smith, D. R. *Science* **2006**, *312* (5781), 1780–1782.
- (6) Schurig, D.; Mock, J. J.; Justice, B. J.; Cummer, S. A.; Pendry, J. B.; Starr, A. F.; Smith, D. R. *Science* **2006**, *314* (5801), 977–980.
- (7) Valentine, J.; Li, J.; Zentgraf, T.; Bartal, G.; Zhang, X. *Nat. Mater.* **2009**, *8* (7), 568–571.
- (8) Wu, C.; Khanikaev, A. B.; Shvets, G. *Phys. Rev. Lett.* **2011**, *106* (10), 1–4.
- (9) Kanté, B.; Park, Y.-S.; O'Brien, K.; Shuldman, D.; Lanzillotti-Kimura, N. D.; Jing Wong, Z.; Yin, X.; Zhang, X. *Nat. Commun.* **2012**, *3*, 1180.
- (10) Ni, X.; Wong, Z. J.; Mrejen, M.; Wang, Y.; Zhang, X. *Science* **2015**, *349* (6254), 1310–1314.
- (11) Lee, H.-J.; Lee, H.-S.; Yoo, K.-H.; Yook, J.-G. *J. Appl. Phys.* **2010**, *108* (1), 014908.
- (12) Xu, X.; Peng, B.; Li, D.; Zhang, J.; Wong, L. M.; Zhang, Q.; Wang, S.; Xiong, Q. *Nano Lett.* **2011**, *11* (8), 3232–3238.
- (13) Lim, S.; Caloz, C.; Itoh, T. *IEEE Trans. Microwave Theory Tech.* **2005**, *53* (1), 161–173.
- (14) Padilla, W. J.; Taylor, A. J.; Highstrete, C.; Lee, M.; Averitt, R. D. *Phys. Rev. Lett.* **2006**, *96* (10), 107401.
- (15) Driscoll, T.; Palit, S.; Qazilbash, M. M.; Brehm, M.; Keilmann, F.; Chae, B.-G.; Yun, S.-J.; Kim, H.-T.; Cho, S. Y.; Jokerst, N. M.; Smith, D. R.; Basov, D. N. *Appl. Phys. Lett.* **2008**, *93* (2), 024101.
- (16) Yang, S.; Ni, X.; Yin, X.; Kante, B.; Zhang, P.; Zhu, J.; Wang, Y.; Zhang, X. *Nat. Nanotechnol.* **2014**, *9* (12), 1002–1006.
- (17) Kuzyk, A.; Schreiber, R.; Zhang, H.; Govorov, A. O.; Liedl, T.; Liu, N. *Nat. Mater.* **2014**, *13* (9), 862–866.
- (18) Macfarlane, R. J.; Jones, M. R.; Lee, B.; Auyeung, E.; Mirkin, C. A. *Science* **2013**, *341* (6151), 1222–1225.
- (19) Mason, J. A.; Laramy, C. R.; Lai, C. T.; O'Brien, M. N.; Lin, Q. Y.; Dravid, V. P.; Schatz, G. C.; Mirkin, C. A. *J. Am. Chem. Soc.* **2016**, *138* (28), 8722–8725.
- (20) Douglas, S. M.; Bachelet, I.; Church, G. M. *Science* **2012**, *335* (6070), 831–834.
- (21) Maye, M. M.; Kumara, M. T.; Nykypanchuk, D.; Sherman, W. B.; Gang, O. *Nat. Nanotechnol.* **2010**, *5* (2), 116–120.
- (22) Pal, S.; Zhang, Y.; Kumar, S. K.; Gang, O. *J. Am. Chem. Soc.* **2015**, *137* (12), 4030–4033.
- (23) Zhang, S.; Genov, D. A.; Wang, Y.; Liu, M.; Zhang, X. *Phys. Rev. Lett.* **2008**, *101* (4), 47401.
- (24) Liu, N.; Langguth, L.; Weiss, T.; Kästel, J.; Fleischhauer, M.; Pfau, T.; Giessen, H. *Nat. Mater.* **2009**, *8* (9), 758–762.
- (25) Zentgraf, T.; Zhang, S.; Oulton, R. F.; Zhang, X. *Phys. Rev. B: Condens. Matter Mater. Phys.* **2009**, *80* (19), 195415.
- (26) Liu, M.; Hwang, H. Y.; Tao, H.; Strikwerda, A. C.; Fan, K.; Keiser, G. R.; Sternbach, A. J.; West, K. G.; Kittiwatanakul, S.; Lu, J.; Wolf, S. A.; Omenetto, F. G.; Zhang, X.; Nelson, K. A.; Averitt, R. D. *Nature* **2012**, *487* (7407), 345–348.
- (27) Pryce, I. M.; Aydin, K.; Kelaita, Y. A.; Briggs, R. M.; Atwater, H. A. *Nano Lett.* **2010**, *10* (10), 4222–4227.
- (28) Chen, H.-T.; O'Hara, J. F.; Azad, A. K.; Taylor, A. J.; Averitt, R. D.; Shrekenhamer, D. B.; Padilla, W. J. *Nat. Photonics* **2008**, *2* (5), 295–298.
- (29) Ju, L.; Geng, B.; Horng, J.; Girit, C.; Martin, M.; Hao, Z.; Bechtel, H. A.; Liang, X.; Zettl, A.; Shen, Y. R.; Wang, F. *Nat. Nanotechnol.* **2011**, *6* (10), 630–634.
- (30) Alivisatos, A.; Johnsson, K.; Peng, X.; Wilson, T. E.; Loweth, C. J.; Bruchez, M. P. J.; Schultz, P. G. *Nature* **1996**, *382* (15), 609–611.
- (31) Mirkin, C.; Letsinger, R.; Mucic, R.; Storhoff, J. *Nature* **1996**, *382* (15), 607–609.
- (32) Jones, M. R.; Seeman, N. C.; Mirkin, C. A. *Science* **2015**, *347* (6224), 1260901–1260901.
- (33) Mastroianni, A. J.; Claridge, S. A.; Alivisatos, A. P. *J. Am. Chem. Soc.* **2009**, *131* (24), 8455–8459.
- (34) Li, Y.; Liu, Z.; Yu, G.; Jiang, W.; Mao, C. *J. Am. Chem. Soc.* **2015**, *137* (13), 4320–4323.
- (35) Sönnichsen, C.; Reinhard, B. M.; Liphardt, J.; Alivisatos, A. P. *Nat. Biotechnol.* **2005**, *23* (6), 741–745.
- (36) Jun, Y.-W.; Sheikholeslami, S.; Hostetter, D. R.; Tajon, C.; Craik, C. S.; Alivisatos, A. P. *Proc. Natl. Acad. Sci. U. S. A.* **2009**, *106* (42), 17735–17740.
- (37) Lee, S. E.; Chen, Q.; Bhat, R.; Petkiewicz, S.; Smith, J. M.; Ferry, V. E.; Correia, A. L.; Alivisatos, A. P.; Bissell, M. J. *Nano Lett.* **2015**, *15* (7), 4564–4570.
- (38) Reinhard, B. M.; Sheikholeslami, S.; Mastroianni, A.; Alivisatos, A. P.; Liphardt, J. *Proc. Natl. Acad. Sci. U. S. A.* **2007**, *104* (8), 2667–2672.
- (39) Auyeung, E.; Cutler, J. I.; Macfarlane, R. J.; Jones, M. R.; Wu, J.; Liu, G.; Zhang, K.; Osberg, K. D.; Mirkin, C. A. *Nat. Nanotechnol.* **2012**, *7* (1), 24–28.
- (40) Kuzyk, A.; Schreiber, R.; Fan, Z.; Pardatscher, G.; Roller, E.-M.; Högele, A.; Simmel, F. C.; Govorov, A. O.; Liedl, T. *Nature* **2012**, *483* (7389), 311–314.
- (41) Urban, M. J.; Dutta, P. K.; Wang, P.; Duan, X.; Shen, X.; Ding, B.; Ke, Y.; Liu, N. *J. Am. Chem. Soc.* **2016**, *138* (17), 5495–5498.
- (42) Liu, N.; Weiss, T.; Mesch, M.; Langguth, L.; Eigenthaler, U.; Hirscher, M.; Sönnichsen, C.; Giessen, H. *Nano Lett.* **2010**, *10* (4), 1103–1107.
- (43) Liu, N.; Hentschel, M.; Weiss, T.; Alivisatos, A. P.; Giessen, H. *Science* **2011**, *332* (6036), 1407–1410.
- (44) Garrido Alzar, C. L.; Martinez, M. a. G.; Nussenzeig, P. *Am. J. Phys.* **2002**, *70* (1), 37.
- (45) Halas, N. J.; Lal, S.; Chang, W.-S.; Link, S.; Nordlander, P. *Chem. Rev.* **2011**, *111* (6), 3913–3961.
- (46) Gallinet, B.; Siegfried, T.; Sigg, H.; Nordlander, P.; Martin, O. J. F. *Nano Lett.* **2013**, *13* (2), 497–503.
- (47) Davis, T. J.; Hentschel, M.; Liu, N.; Giessen, H. *ACS Nano* **2012**, *6* (2), 1291–1298.
- (48) Flauraud, V.; Bernasconi, G. D.; Butet, J.; Mastrangeli, M.; Alexander, D. T. L.; Martin, O. J. F.; Brugger, J. *ACS Photonics* **2017**, *4* (7), 1661–1668.
- (49) Lang, D.; Taylor, T. N.; Doby, D. C.; Gray, D. M. *J. Mol. Biol.* **1976**, *106* (1), 97–107.
- (50) Radha, B.; Senesi, A. J.; O'Brien, M. N.; Wang, M. X.; Auyeung, E.; Lee, B.; Mirkin, C. A. *Nano Lett.* **2014**, *14* (4), 2162–2167.
- (51) Aydin, K.; Ferry, V. E.; Briggs, R. M.; Atwater, H. A. *Nat. Commun.* **2011**, *2*, 517.
- (52) Kern, A. M.; Martin, O. J. F. In *SPIE Proceedings*; Kawata, S., Shalae, V. M., Tsai, D. P., Eds.; SPIE, 2009; Vol. 7395, p 739518.
- (53) Jin, R.; Wu, G.; Li, Z.; Mirkin, C. A.; Schatz, G. C. *J. Am. Chem. Soc.* **2003**, *125* (6), 1643–1654.
- (54) Lee, C. H.; Mizusawa, H.; Kakefuda, T. *Proc. Natl. Acad. Sci. U. S. A.* **1981**, *78* (5), 2838–2842.
- (55) Macfarlane, R. J.; Jones, M. R.; Senesi, A. J.; Young, K. L.; Lee, B.; Wu, J.; Mirkin, C. A. *Angew. Chem., Int. Ed.* **2010**, *49* (27), 4589–4592.